Mineralogical Magazine, August 2007, Vol. 71(4), pp. 461–476

Metamorphic effects on agate found near the Shap granite, Cumbria, England: as demonstrated by petrography, X-ray diffraction and spectroscopic methods

T. MOXON[1,*], S. J. B. REED[2] AND M. ZHANG[2]

[1] 55 Common Lane, Auckley, Doncaster DN9 3HX, UK
[2] Department of Earth Sciences, University of Cambridge, Downing Street, Cambridge CB2 3EQ, UK

[*Received 18 June 2007; Accepted 18 December 2007*]

ABSTRACT

Agates from a 430 Ma host at Stockdale Beck, Cumbria, England have been characterized. The crystallite size of the Stockdale Beck agates was found to be ~60% greater than any other agates from five regions aged 400–1100 Ma. Raman spectroscopy identified moganite in all agates tested except those from Stockdale Beck. Infrared spectroscopy showed that the silanol content of the Stockdale Beck agates was near zero. The properties of agates from Stockdale Beck and the 1.84–3.48 Ga metamorphosed hosts found in Western Australia were similar but different from agates found in other hosts aged 400–1100 Ma. Cathodoluminescence demonstrates further differences between agates from hosts aged 13–1100 Ma and those from Stockdale Beck and Western Australia. Agates from the latter areas have a lower proportion of defects causing a red emission band (~660 nm) but an increased proportion of defects causing blue (~470 nm) and orange (~640 nm) emission bands. Agates found in hosts aged 13–1100 Ma are also differentiated from the Stockdale Beck and Western Australian agates in a ternary plot of the relative intensities of violet to blue to orange emission bands. Single scans producing this combination of colours are only found in the Stockdale Beck and Western Australian agates. The properties shown by the Stockdale Beck and Western Australian agates demonstrate that an agate or chalcedony infill can be used to identify post-deposition palaeoheating within a host rock.

KEYWORDS: agate, chalcedony, moganite, IR, Raman, XRD, cathodoluminescence.

Introduction

CHALCEDONY is a variety of microcrystalline α-quartz that generally displays a fibrous texture under the polarizing microscope. Agate is banded chalcedony that is sometimes formed as a cavity infill within an igneous environment. The most frequently seen banding in agates is a repetitive wall-lining of gas vesicles that creates a series of onion-like layers. Moxon (1991) attributed the banding to various causes. Optical and electron microscopy showed that the white bands were composed of a plate-edge-like texture that reflected incident light but scattered transmitted light. The rhythmic deposition of Fe oxide spots produced red and yellow banding. Thin sections of agates can show continuous breaks at right angles to the fibrous growth thus creating fine banding. Horizontally formed bands, implying gravity control, are only found in a limited number of agate regions. Agates are deposited world-wide within a variety of volcanic rocks but sedimentary and metamorphic agate hosts are much rarer.

Agate has very high silica purity with non-volatile impurities being <1% (Flörke *et al.*, 1982). The major impurity in agate is the total water (free H_2O and defect-site silanol Si–OH) with a concentration of up to 2% (Graetsch *et al.*, 1985). However, most agate is a mixture of two silica polymorphs: moganite and α-quartz. The

* E-mail: moxon.t@tiscali.co.uk
DOI: 10.1180/minmag.2007.071.4.461

crystal structure of moganite has been described as the alternate stacking of layers of left- and right-handed quartz on the unit-cell scale (Miehe and Graetsch, 1992). The moganite content in igneous-hosted agate and chalcedony varies from zero (Moxon *et al*., 2006) to ~70% (Parthasarathy *et al.*, 2001; Pop *et al*., 2004). It has been demonstrated that the moganite content and defect-site water in agates decreases over the first 400 Ma while the crystallite size of α-quartz increases (Moxon and Ríos, 2004). A good correlation was shown between agate crystallite size and the age of host rocks <400 Ma. Brazilian and Northumbrian agates were exceptions and it was proposed that they were formed during known later periods of volcanic activity (Moxon and Ríos, 2004). In general, the formation of wall-lining agates can be regarded as occurring within a few million years of the host. The crystallite size and the defect-site water content were shown to be approximately constant in agates from hosts aged 400−1100 Ma. It was argued that the cessation of crystallite growth is due to the completion of a moganite → chalcedony transformation.

Stockdale Beck, Cumbria, England is ~5 km from the Shap granite and the Stockdale Beck agates were examined in order to determine whether the later granite intrusion had affected the physical properties. These Cumbrian agates were compared with agates from other locations around the world with emphasis given to similarly-aged hosts. In addition to the changes produced by low-temperature ageing, agates can also be affected by thermal events. A study of agates from the metamorphosed hosts of the Pilbara Craton, Western Australia showed an advanced crystallization, zero moganite and in some cases a partial breakdown in the fibrous chalcedony (Moxon *et al*., 2006). The agates in this study have been characterized using a variety of techniques: X-ray diffraction (XRD) to assess crystallinity, optical and scanning electron microscopy (SEM) to assess microstructure, cathodoluminescence (CL) to assess structural defects, Raman spectroscopy to assess the moganite content and infrared (IR) spectroscopy to assess the water content. Throughout the paper, the numbers in parentheses are ± one standard deviation.

Stockdale Beck agate host rocks

These agates occur in a small area in the Stockdale Beck, Longsleddale, Cumbria, England. The agate-parent rocks were formed in the last major volcanism after the formation of the Borrowdale Volcanic Group. However, both the nature and age of the hosts have proven to be problematic.

Early accounts of the host rock considered a rhyolite lava flow as the most likely origin (Gale *et al*., 1979). However, after a detailed re-assessment of the agate hosts by Millward and Lawrence (1985), they concluded that the observed textures are more indicative of welded tuff and ought to be regarded as a rheomorphic ignimbrite.

Two fist-sized samples of host rock were collected at Stockdale Beck and sliced. Both contained a mixture of host (h), hematite banding in agate (ag) and chalcedony (ch) (Fig. 1*b*); one sample also contained milky macrocrystalline quartz. These two rock sections show that agate or brown chalcedony has filled all available spaces within the host rock, giving the impression of a simultaneous deposition of host and agate. This silica infill of the Stockdale Beck host is unusual and contrasts with the typical igneous amygdales illustrated by samples found in weathered basalt from the Isle of Mull (Fig. 1*d*).

Gale *et al*. (1979), using the Rb-Sr method, determined the agate-host age at 421± 3 Ma. A re-examination of the same data by Compston *et al*. (1982) suggested that the Stockdale Beck host is at least 430±7 Ma; this date will be used in the later discussion. The nearby Shap granite has been dated at 394±3 Ma (Wadge *et al*., 1978).

Agate samples

Stockdale Beck agates

The Stockdale Beck agates used in the study are separate fragments, whole nodules and agate removed from the two samples of host rock. The agates have poor banding and can be classified primarily into two types. One group has a grey translucency and is mainly band-free chalcedony (Fig. 1*a*); a second type has faint hematite bands. All the Stockdale Beck agates examined lack the more intense regular rhythmic wall-lining bands typified by a Mexican agate shown in Fig. 1*c*.

Reference agates

Agates from hosts aged 400−1100 Ma have an approximately constant density, crystallite size

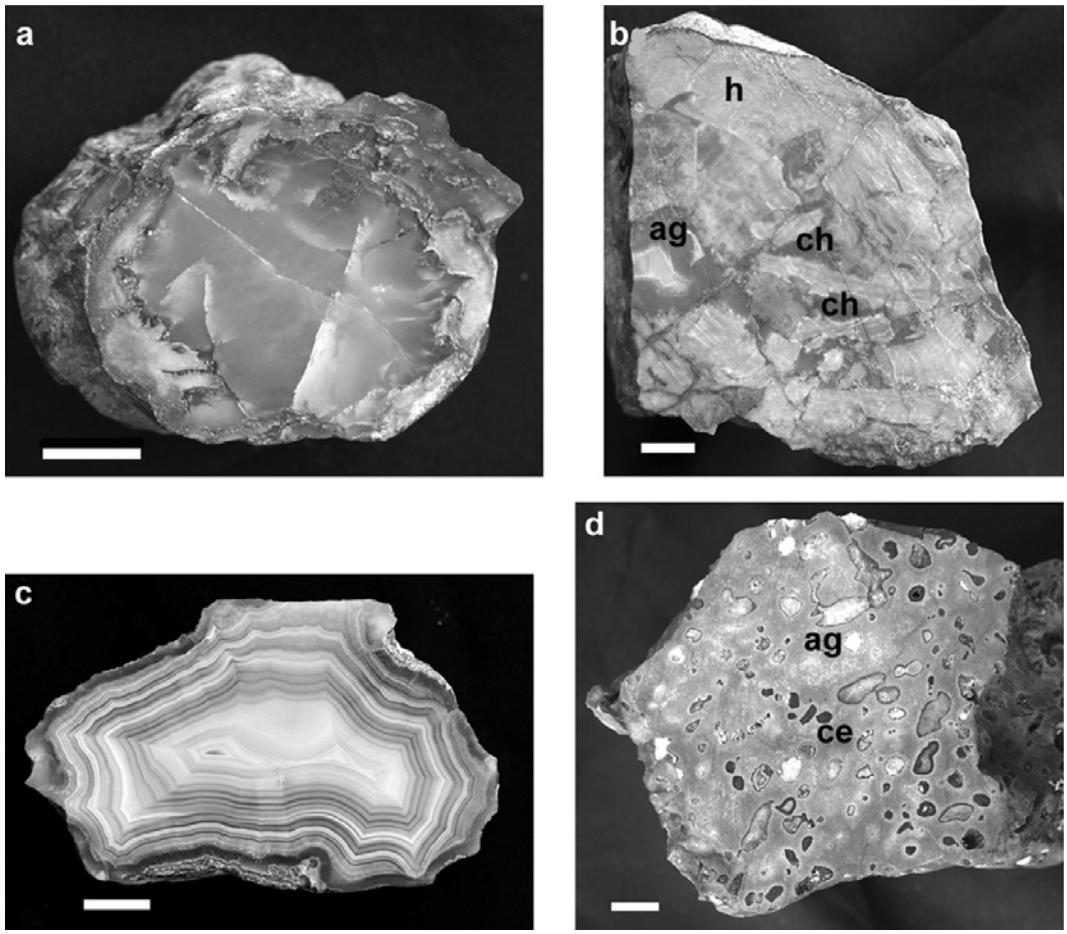

FIG. 1. (*a*) A sliced Stockdale Beck nodule revealing grey chalcedony. (*b*) Sectioned host rock from Stockdale Beck showing: agate (ag), host rock (h) and brown chalcedony (ch). (*c*) Wall-lining agate from Chihuahua, Mexico. (d) Typical small amygdales found in a basalt host, Isle of Mull, Scotland: agate (ag) and celadonite (ce) are shown. The Isle of Mull sample shows celadonite as both an outer covering of agate and an infill of empty gas vesicles. Scale bars: 1 cm.

and defect-site water and a small moganite content (Moxon and Ríos, 2004; Moxon *et al*., 2006). Agates from five different regions aged 400–1100 Ma provided comparative material for the 430 Ma Stockdale Beck samples. A further suite of agates from hosts aged 13–391 Ma were added to the older samples for a CL investigation. Samples from Woolshed Creek Hut, Canterbury, New Zealand, were from a similar host rock: an 89 Ma ignimbrite (Barley *et al*., 1988). A previous study has shown that post-deposition heating can alter the character of agates (Moxon *et al*., 2006). Agates from the 1.84 Ga hosts in the Yerrida Basin and from the 2.72 Ga and 3.48 Ga hosts in the Pilbara Craton, Western Australia, provided samples that had been subjected to low-grade metamorphism. A list of the agates used in the study is given in Table 1.

Experimental methods

Petrography

Around 30 thin sections of whole agates cut approximately parallel to the fibrous growth were used for general petrographic comparisons with the agates of Stockdale Beck.

TABLE 1. Agate samples used for [a]XRD , [b]Raman, [c]IR and [d]CL.

Region	Age of host (Ma)	Site and sample number (Collectors named in acknowledgements)	
1. Yucca Mt., USA**	13*[3]	Yucca Mt., HD 2257[d]	(LN)
2. Mt Warning, Queensland, Australia	23*[3]	Oxley River, 2[d], 3[a], 4[d], 5[a], 7[d], 9[d]	(JRi)
3. Chihuahua, Mexico	38*[4]	Ojo Laguna, 1[d], 2[a], 4[a], 5[ad], 10[d], 13[d]	(BC)
4. Las Choyas. Mexico	45*[5]	Las Choyas, 1[ab], 3[ab]	(BC, JC)
5. Khur, Iran	50*[1]	Khur, 7[d], 31[d], 33[d], 49[a]	(MN)
6. British Tertiary Volcanic Province	60*[1]	Mull, 2[d], 11[a],14[d]; Rum, 5[d], 12[d], 15[d],17[a]	(BT, RL)
7. Mt Somers, Canterbury, New Zealand	89*[6]	Woolshed, 1[c,d], 4[bd], 16[c]	(RB, VT)
8. Rio do Sul, Brazil	133*[1]	Soledado Mines, B21[d], 25[d], 31[d], 33[d], 36[d], 54[ad], 60[bd], 62[d], 64[d], 85[b]	(purchased)
9. Semolale, Botswana,	180*[3]	Bobonong, 70[a], 80[d], 85[ad], 101[d], 110[d], 120[d]	(HK)
10. Agate Creek, Queensland, Australia	275*[1]	Agate Creek, 16[d], 65[d], 76[d], 104[d], 109[a], 129[d]	(NC)
11. Thuringia, Germany	285*[1]	Thuringia Forest, Th 3[a], 4[d], 9[a]	(GH)
12. Northumbria, England	391*[1]	R Breamish, N11[b], 16[b], 17[a], 22[a], 24[a], 32[a], 49[d]	(TM, NC)
13. Eastern Midland Valley, Scotland	412*[1]	Barras Q, 1[d]; Glenfarg, 1[a]; Montrose, 9[a], 10[a]; Ethiebeaton Q, 11[ad], 17[a], 37[ad], 44[a], 111[d]; Ardownie, 7[a]; Scurdie, 1[a]	(BW, BL, TM)
14. Western Midland Valley, Scotland	412*[1]	Carrick Hills, BC 1[a], 2[a], 5[a], 10[a], 9[d], 20[b]; B. Anne, 1[d], 3[d]; Galston, 1[cd]; Glenburn, 3[d], 4[cd]; Dunure, 2[b], 20[d]; Strathern, 1[a]; Maidens, 1[a]	(JRa, TM)
15. Shap, Cumbria, England	430*[7]	Stockdale Beck, 1[a], 2[ad], 3[abcd], 4[a], 5[abd], 6[a], 7[d], 10[bcd], 12[ad], 21[a], 22[ac]	(TM)
16. Northern Territory, Australia	513*[2]	Antrim basalts, 1[a], 2[a], 3[a], 4[a], 5[ad], 6[a]	(JRi)
17. Maydena, Tasmania	515*[2]	Maydena, 1[a], 2[a], 4[a], 5[a], 7[a], 11[a]	(JRi)
18. Lake Superior, USA	1100*[1]	Lincoln, 1[ad], 3[a], 4[abd], 8[d]; Minneapolis, 10[ac], 11[a], 12[abd], 13[a], 14[ad]	(BC, SW, JZ)
19. Yerrida Basin, Western Australia	1840*[3]	Killara Formation, 1[a], 2[a], 3[a], 4[ad], 5[a], 6[d]	(DN)
20. Pilbara, Western Australia**	2720*[3]	Maddina Basalt, 1[ad]	(DN)
21. Pilbara, Western Australia**	3480*[3]	Warrawoona Group, 1[ad], 2[a]	(DN)

Age references are given in *[1] Moxon (2002), *[2] Moxon and Ríos (2004), *[3] Moxon *et al.* (2006), *[4] Moxon and Reed (2006), *[5] Keller *et al*. (1982), *[6] Barley *et al*. (1988), *[7] Compston *et al*. (1982)
** Agates from these areas were limited in availability.

X-ray diffraction

Measurements of accurate powder XRD intensities require a grain size of <10 μm (Bish and Reynolds, 1989). Each agate powder was hand ground and passed through a <52 μm sieve. A fixed mass of the sieved powder was held in a suspension of ethanol and ground by ball mill. Samples of the powders were examined optically and shown to be in the 4–10 μm range.

A Bruker D8 diffractometer with Cu-$K\alpha$ radiation was used in reflection mode. Initial XRD runs were used for mineral identification over the 16–52º2θ range with a step size of 0.02º2θ. To estimate crystallite size, separate runs were used to calculate the full width at half maximum (FWHM) of the 101 quartz reflection at 26.64º2θ with a scan over the 16–30º2θ range and a step size of 0.01º. Corrections for instrumental broadening were made with added Si as an internal standard. Around 40 reference agates from the metamorphosed hosts of Western Australia, hosts aged 400–1100 Ma, together with eight whole and fragmentary Stockdale Beck agates were investigated.

A final set of XRD runs was obtained over the 66–69º2θ range with a step size of 0.02º2θ for 20 s/step. Microcrystalline quartz shows peak

broadening over this high 2θ range. These runs were used to determine the Crystallinity Index (CI) based on the relative intensity of the peak of the 212 reflection to the trough between the 212 and 203 reflections: this ratio is compared to a euhedral quartz reference. Colourless Brazilian macrocrystalline quartz, used as a standard in the XRD laboratory at Cambridge University, was the CI reference material. Madagascan rose quartz and Scottish amethyst were also investigated as possible standards.

Klug and Alexander (1974) investigated XRD intensity reproducibility using a variety of quartz powders of various sizes. They reported mean percentage intensity deviations of 18.2% and 1.2% for powders 15–50 μm and <5 μm, respectively. However, the poor crystallinity in young agates leads to very broad reflections with considerable overlap at this high 2θ angle. In order to get a measurable 212 signal from the immature agates, coarser powders were used. For these CI experiments, powders were sieved to <52 μm and lightly ground under ethanol.

Raman spectroscopy

In this study, the main aim in using Raman spectroscopy was to identify moganite and quartz in agates from similarly aged agate hosts. Raman spectra were excited by the 623 nm line of a Ne-He laser and collected with a free-sample-space LabRam micro-Raman spectrometer. Instrument calibrations were carried out using a silicon wafer. The spectra were recorded in backscattering geometry with a spectral resolution of 4 cm^{-1} and spatial resolution of ~1 μm. A CCD detector, plus grating (1800 grooves/mm), plus 50× and 100× objectives were coupled to the free-space microscope. All measurements were at room temperature. Slabs of agate were cut approximately parallel to the fibrous growth and ground flat using F 600 silicon carbide grit. The agates were scanned for Raman shifts between 200 and 1100 cm^{-1}. A minimum of six scans were recorded on representative parts of each agate including banded and nearby non-banded areas.

Infrared spectroscopy

A Bruker IFS 113v Fourier transform infrared spectrometer equipped with an IRscope-II infrared microscope was used to record absorption spectra between 2000 and 7000 cm^{-1} at an instrumental resolution of 4 cm^{-1}. A liquid-nitrogen-cooled MCT detector was chosen to couple with a KBr beam splitter and a Globar source. The beam size was set at 60–80 μm and the spectra were averaged over 100 scans. Several agate sections, ~100–150 μm thick, were polished on both sides and examined using the spectrometer in transmission mode.

Scanning electron microscopy

A standard scanning electron microscopy (SEM) technique was used with small, freshly fractured agate fragments being coated with gold and examined at 20 kV with a current of ~1 nA. Several micrographs of various agates were taken at magnifications of 200–5000×.

Cathodoluminescence

All the Stockdale Beck agate samples used for CL were standard polished thin sections, thinly coated with gold. Cathodoluminescence spectra were recorded with a Gatan MonoCL3 system consisting of a paraboloidal light-collecting mirror, a grating spectrograph and multiplier detector, attached to a JEOL 820 scanning electron microscope, using the following conditions: accelerating voltage – 20 kV, beam current ~10 nA, spot size ~10 μm. Spectra were recorded digitally over a wavelength range of 200–900 nm with a step size of 10 nm and a dwell time of 1 s. After background subtraction (based on the count-rate observed in the 200–250 nm region where the light intensity was zero), the spectra were corrected for detection efficiency with wavelength as determined with a standard tungsten lamp.

It is known that changes in CL spectra commonly occur as a result of electron bombardment. This effect on agate has been investigated previously (Moxon and Reed, 2006). No changes in the wavelengths of the emission bands from repeated wavelength scans were observed. However, the violet:red intensity ratio showed a 7% increase from first to second scan. Throughout this study, the electron bombardment effect was minimized by carrying out repeated scans at different points. The CL variations within a single agate have been investigated previously using three selected agates which were systematically scanned at equidistant points N→S and W→E (Moxon and Reed, 2006). Apart from one area, where the agate showed complex banding, little difference between the relative intensities was obtained.

Results

Petrography

Although chalcedony is described as showing fibrous growth under the polarizing microscope, the orientation and nature of the fibres can be complex. Braitsch (1957) and Frondel (1978) carried out wide-ranging surveys of the fibres in chalcedony and found that the most common growth direction is parallel to 110. More recently, Cady *et al*. (1998) discussed the complex fibre variation during growth and used quantitative X-ray texture analysis to identify fibre elongation. The typical wall-lining chalcedonic growth is shown in a Mexican agate having a clear chalcedony outer band and a contrast in texture shown by the yellow centre (Fig. 2*d*).

Thin sections of the Stockdale Beck agates show unusual textures (Fig. 2*a*–*c*). All have some area that is recognizable as chalcedony, e.g. the first band in Fig. 2*c*, but the texture in the rest of the agate resembles iron filings under the influence of a magnetic field. The right-hand deposit in Stockdale Beck (sample No 7, Fig. 2*b*, ii) does show a good example of chalcedonic fibrosity that contrasts with the surrounding host (h).

X-ray diffraction

The only crystalline phase identified in the Stockdale Beck agate samples was α-quartz. Four different agate powders were used to investigate the possibility of a ball-mill-created amorphization. The diffuse signal over the 15 to

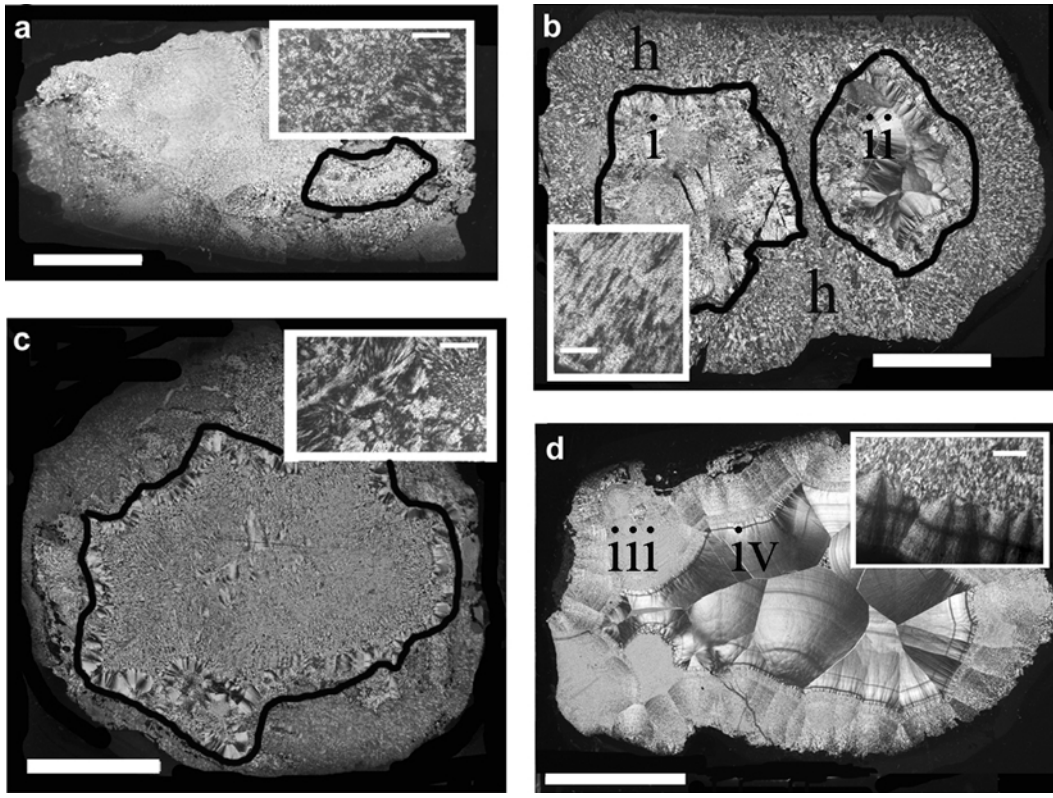

FIG. 2. Unusual textures are shown by the thin sections of Stockdale Beck agates (*a*–*c*): these textures are in contrast with the typical chalcedonic fibrous growth in a Mexican agate (*d*). (*b*) (i) and (ii) show a twin nodule growth with different textures in the same slab from Stockdale Beck (sample 7). These agates are surrounded by host rock (h). (*d*) Mexican agate showing textural differences between the colourless (iii) and final yellow regions (iv). The chalcedony has been highlighted in the Stockdale Beck agates. Inserts show the chalcedony at a higher magnification. Scale bars, main: 1 cm; insert: 1 mm.

33º2θ range showed negligible differences between the <52 μm hand-ground powders and the ball-mill ground powders.

The mean crystallite size was estimated from XRD peak widths. At least six samples per locality were used for all crystallite-size determinations except the Archaean agates from Western Australia, where only one and two samples, respectively, from Maddina and Warrawoona were available. The method used for estimation of crystallite size ($C_{s(101)}$) was based upon the 101 quartz reflection. The determination of $C_{s(101)}$ used the FWHM (βq) of diffraction maxima together with FWHM (βs) of Si at 28.44º2θ for instrument-broadening corrections. The shape factor (K) was taken as unity and, together with the wavelength λ (Cu-$K\alpha$), was utilized to calculate $C_{s(101)}$ in the Scherrer equation: $C_{s(101)} = K\lambda/(\cos\theta).\sqrt{(\beta q^2 - \beta s^2)}$. The crystallite size of the tested agates found in hosts of age >400 Ma is given in Table 2. The mean value of $C_{s(101)}$ found in eight Stockdale Beck agates was 1906 (224) Å. Agates from hosts aged 400−1100 Ma gave a mean $C_{s(101)}$ between 923 and 1214 Å in each of the five regions (Table 2). An upper limit of measurable $C_{s(101)}$ using XRD was found to be ~2000 Å. This limit of crystallite-size determination is reached when the FWHM of the internal standard approaches the FWHM of the agate. All the Proterozoic and Archaean Western Australian agates produced the largest crystallite size: >2000 Å. These agate hosts have been subjected to low-grade metamorphism and the crystallite growth in the agates from the oldest hosts is probably due to burial during the Proterozoic: ~2.00 and 2.45 Ga (Nelson *et al*., 1992).

Previous works (Moxon *et al*., 2006; and the cited literature therein on crystallinity) used a Huber 641 diffractometer in transmission mode for calculating crystallite size. Here, a Bruker D8 diffractometer was used in reflection mode. A number of samples from the same agates was examined by both instruments. The determined crystallite size of agates from hosts aged 400−1100 Ma showed machine differences with crystallite sizes in the Bruker D8 being ~75% greater. All data shown in Table 2 were obtained using the Bruker D8.

Murata and Norman (1976) devised the Crystallinity Index (CI) for the microcrystalline quartz minerals based upon peak resolution in the 212 reflection at 67.74º2θ. The height of peak *a* is first divided by the total height above background *b* (Fig. 3*d*). The Crystallinity Index is defined as: CI = 10F*a*/*b* where F is the scaling factor determined by a macrocrystalline quartz standard. This provides a CI arbitrary scale of 1 to 10. Brazilian macrocrystalline quartz, Madagascan rose quartz and Scottish amethyst were investigated to examine any variation between different types of macrocrystalline quartz standards. Minimal differences were found: Brazilian macrocrystalline quartz was selected as the nominal standard to be equal to 10; hence rose quartz = 10.1 and amethyst = 9.6.

Moxon *et al*. (2006) determined the CI of ~100 agates using a Huber 641 diffractometer in transmission mode. They found that the CI data could be broadly considered as belonging to three groups produced by agates from hosts <180 Ma, 180−1100 Ma and the metamorphosed hosts of Western Australia agate. Around 40 samples

TABLE 2. Variation in the crystallite size ($C_{s\,101}$) with age of the host rock.

Region	Age of host (Ma)	Mean crystallite size (Å) (±σ)
1. East Midland Valley, Scotland	412	923 (202)
2. West Midland Valley, Scotland	412	990 (157)
3. Stockdale Beck, England	430	1906 (224)
4. Northern Territory, Australia	513	1060 (67)
5. Maydena, Tasmania	488−542*	1214 (121)
6. Lake Superior, USA	1100	961 (141)
7. Killara, Yerrida Basin, Western Australia**	1840	>2000
8. Maddina, Western Australia**	2720	>2000
9. Warrawoona, Western Australia**	3480	>2000

* Sheet 4626-Tasmanian Geological Survey lists the hosts as Cambrian.
** The Western Australian agates are found in hosts that have undergone low-grade metamorphism.

including some agates from the 2006 study have been re-examined with the Bruker D8. Again, this instrument gave much sharper reflections but produced the same three major age-related divisions with CI of 4.4(1.6), 6.9(1.1) and 9.9(0.1) for the three respective groups. The large standard deviation in the younger agates is due to the low reflection intensity combined with the use of the <52 μm powders. The CI for the Stockdale Beck agates was 9.7(0.1). Agates used for CI determination are given in Table 1 and individual sample plots are shown in Fig. 3.

Scanning electron microscopy

There have been few studies of the surface morphology of agates using SEM, although detailed examination of German agates showed the surface to be globular (Lange *et al.*, 1984; Holzhey, 1999). A more recent SEM investigation (Moxon, 2002) showed that the globulites in non-white bands produced an approximately age-related growth: the small globules increased in size with the oldest agates often showing a pebble-like surface. The observed petrographic fibrosity was not identified in any of the above SEM studies. However, it was suggested that a series of flat areas identified using the transmission electron microscope (TEM) were due to the chalcedonic fibrosity (Moxon, 1991).

Three Stockdale Beck agates were examined and the textures showed only marginal differences between these and other agates in the 400–1100 Ma host-age range. The micrographs from Stockdale Beck and some samples of the older agates show a granular texture with globular overgrowths (Fig. 4).

Infrared spectroscopy

Agates from Stockdale Beck were compared with samples from the West Midland Valley, Scotland (412 Ma), Lake Superior, USA (1100 Ma) and Woolshed Creek, New Zealand (89 Ma). Data from a previous study investigating Western Australian agates were also available (Moxon *et al.*, 2006). The broad peak from 4000 to 2500 cm^{-1} is due to fundamental O–H stretching vibrations (Yamagishi *et al.*, 1997) and the secondary peak at 3585 cm^{-1} is assigned to Si–OH at silanol defect sites (Graetsch *et al.*, 1985). The IR spectra show that the Stockdale Beck and Western Australian agates have near-zero silanol water. In addition, the Western Australian agates also have near-zero free water (Fig. 5 I). Free and silanol water is present in all other tested agates (Fig. 5 II).

Raman spectroscopy

Kingma and Hemley (1994) demonstrated that the ratio of quartz to moganite can be estimated qualitatively from the relative intensities of the strong quartz (465 cm^{-1}) and moganite

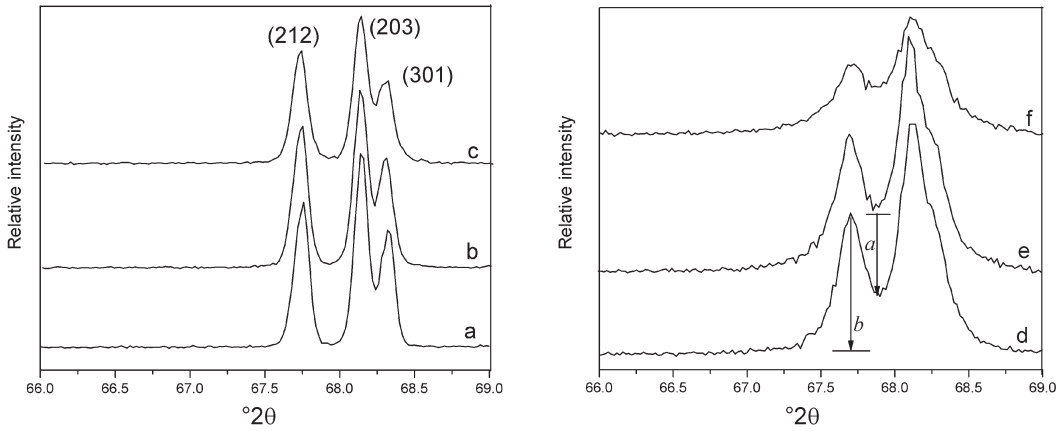

FIG. 3. The increasing crystallinity is shown by the sharpening of the 212, 203 and 301 reflections in agate and macrocrystalline quartz. Locality and age of host: a: Brazilian macrocrystalline quartz reference; b: Warrawoona, Western Australia (3.48 Ga); c: Stockdale Beck, England (430 Ma); d: West Midland Valley, Scotland (412 Ma); e: Agate Creek, Australia (275 Ma); f: Chihuahua, Mexico (38 Ma). The ratio *a*:*b* is used in the calculation of the Crystallinity Index.

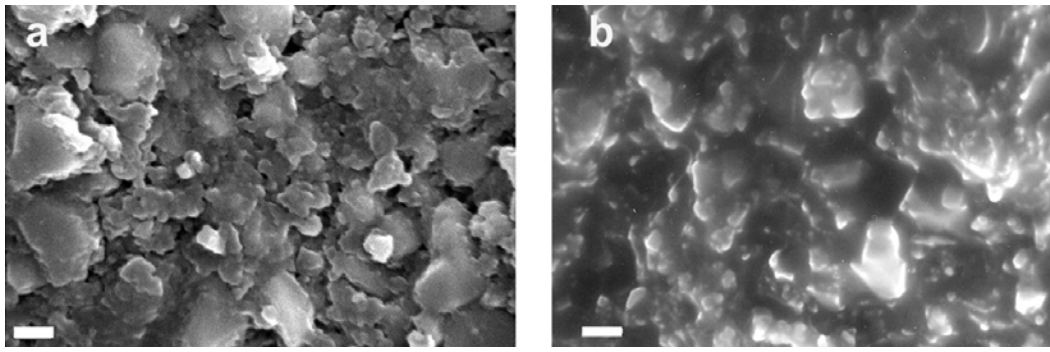

FIG. 4. SEM images of (*a*) Stockdale Beck and (*b*) Lake Superior agates show a similar texture with globular overgrowths. Scale bars: 2 μm

(501 cm^{-1}) peaks in the Raman spectrum. In this study, moganite and quartz were identified in agates from Northumbria, England (391 Ma), West Midland Valley, Scotland (412 Ma), and Lake Superior, USA (1100 Ma) (sample plots are given in Fig. 6). A mean moganite content, based upon the moganite intensity$_{501}$ to quartz intensity$_{465}$, was 5.9(0.6)%, 4.9(0.9)% and 4.8(0.4)%, respectively. The 89 Ma-hosted agates from the New Zealand ignimbrite gave an estimated moganite content of 8.1(0.7)%. Data from these and previous scans (Moxon *et al*. 2006) on other agates show that only the agates from Stockdale Beck and Western Australia were moganite-free (Fig. 6).

Cathodoluminescence

Apart from material from Stockdale Beck, >90 wavelength scans were carried out on agates from igneous hosts. These data were added to the unpublished results from >230 random scans on ~50 igneous-hosted agate slabs and thin sections from an earlier study (Moxon and Reed, 2006). The addition of the extra 90 CL spectra to agates has reduced the standard deviation.

Thin sections of agates show various textures but CL was unable to discriminate between any of the different petrographic features. A minimum of four random scans was used on each agate but all extra scans from attempted links between petrographic observations and CL have been included.

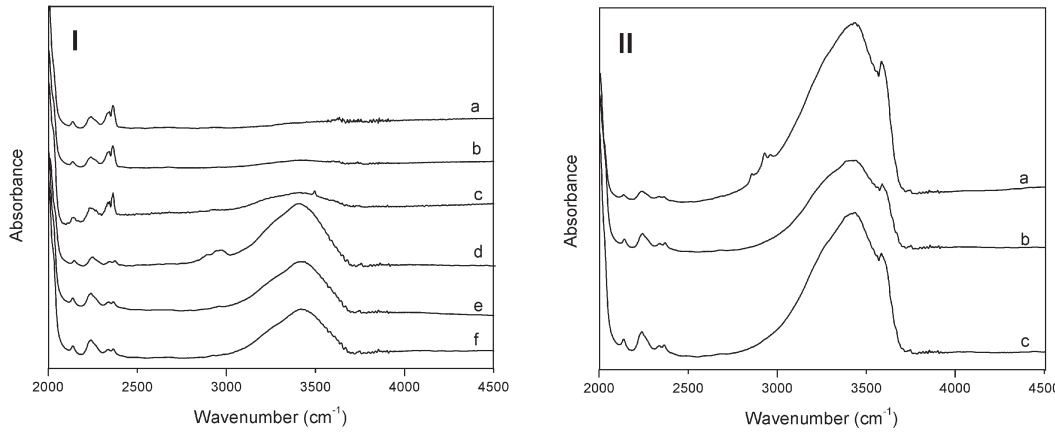

FIG. 5. IR absorption spectra of H_2O and OH in a variety of agates. (I) a: Warrawoona, Western Australia (3.48 Ga); b: Maddina, Western Australia (2.72 Ga); c: Killara, Western Australia (1.84 Ga); d,e,f: three different Stockdale Beck agates (430 Ma). II: Agates from: a: Woolshed Creek, New Zealand (89 Ma); b: West Midland Valley, Scotland (412 Ma); c: Lake Superior, USA (1.10 Ga).

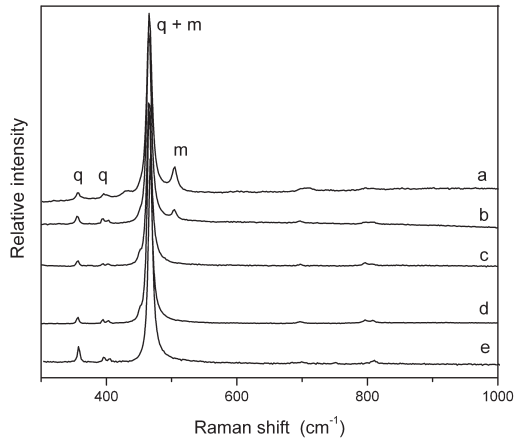

FIG. 6. Raman spectra of agate from (a) Woolshed Creek, New Zealand (89 Ma); (b) West Midland Valley, Scotland (412 Ma); (c) Stockdale Beck, England (430 Ma); (d) Warrawoona, Western Australia (3.48 Ga); (e) Brazilian macrocrystalline quartz. The labelled peaks are the principal spectral peaks of α-quartz (q) and moganite (m).

The CL spectra generally have a Gaussian profile (Stevens Kalceff, 1998). The curve-fitting algorithm in OriginLab's program *Origin* was used to fit three unconstrained Gaussian functions to efficiency-corrected experimental data. The goodness-of-fit shown by the coefficient of determination ($r^2 = 0.97$) was always better than using two Gaussian functions. The fitting into three Gaussian components was used even when a third band was not obvious from a visual inspection. Examples of efficiency-corrected plots are shown in Fig. 7.

The first Gaussian component emission band occurred in either the ultra violet (340−399 nm) or violet (400−450 nm) regions. A total of 444 emission bands were processed and four were outside this 340−450 nm range and classed as outliers. Yellow (540−590 nm) was the predominant colour identified in the second Gaussian component with blue (451−490 nm) and orange (591−648 nm) less common alternatives. There are 19 outliers from the 444 emission bands that are outside the designated wavelengths in this component. Clear distinctions are demonstrated in the second Gaussian component between the Stockdale Beck spectra and those of unheated agates. Agates from the Stockdale Beck produce a blue emission band around three times more frequently than agates from the 13−1100 Ma age range. The third Gaussian component was predominately a red emission band (649−680 nm) as the main colour in agates from hosts aged 13−1100 Ma; orange (591−648 nm) was a lesser alternative. For the Stockdale Beck and Western Australian agates, the red emission band was no longer dominant; no outliers were produced in the third (Table 3). The Gaussian fitting produced two orange emission bands: ~620 nm in the second Gaussian component and ~ 640 nm in the third Gaussian component. These two orange emission bands were never identified in any one scan although each was possible in the same agate.

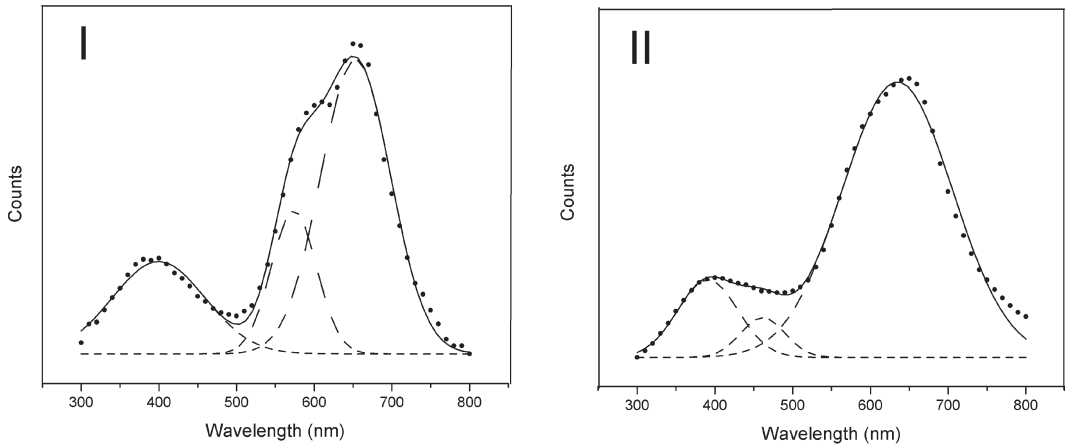

FIG. 7. Efficiency-corrected CL spectrum plots of Stockdale Beck (sample 7). I and II are from the left-and right-hand nodules, respectively, in Fig. 2*b* (solid circles − experimental data; dashed lines − fitted Gaussian components with the sum shown by the solid line).

TABLE 3. Emission bands found in agate and chalcedony.

Region (no of agates tested)	No of scans	First Gaussian component UV 340 399	First Gaussian component Violet 400 450	Second Gaussian component Blue 451 490	Second Gaussian component Yellow 540 590	Second Gaussian component Orange 591 648	Third Gaussian component Orange 591 648	Third Gaussian component Red 649 680
		Wavelength range (nm)						
		Data as a % of each Gaussian component						
Igneous hosts 13−1100 Ma								
Yucca Mt., USA (1)	4	50	50	0	75	25	0	100
Mt. Warning, Australia (4)	22	50	50	[2]*23	41	27	0	100
Chihuahua, Mexico (4)	28	36	64	14	71	15	4	96
Khur, Iran (3)	12	67	33	8	92	0	8	92
British Tertiary Volcanic Province (5)	25	44	56	[2]*16	40	36	4	96
Woolshed Creek, New Zealand (2)	22	64	36	[2]*18	41	32	14	86
Rio do Sul, Brazil (8)	44	41	59	[1]*7	52	39	0	100
Semolale, Botswana (5)	22	68	32	[4]*36	32	14	0	100
Agate Cr., Australia (5)	35	[1]*9	89	[1]*6	80	11	29	71
Thuringia, Germany (1)	4	25	75	25	75	0	0	100
Northumbria, England(1)	7	57	43	0	71	29	0	100
W Midland Valley, Scotland (6)	40	[1]*43	55	[3]*23	65	5	25	75
E Midland Valley, Scotland (4)	31	26	74	0	84	16	19	81
North Terr., Australia (1)	6	100	0	0	50	50	0	100
Lake Sup., USA (5)	20	80	20	20	40	40	0	100
Total = 322 scans								
%		45	54	14	59	23	10	90
Mean wavelength (nm)		380	414	467	565	622	640	665
(s.d.)		15	12	17	17	15	6	7
Stockdale Beck samples								
No. 2	13	54	46	[4]*46	15	8	92	8
No. 3	22	23	77	41	45	14	23	77
No. 5	15	[1]*33	60	13	73	14	60	40
No. 7 (hematite present)	10	50	50	20	80	0	20	80
No. 7 (no hematite)	10	100	0	100	0	0	100	0
No. 8	8	12	88	0	88	12	25	75
No. 10	6	0	100	0	100	0	50	50
No. 12	12	92	8	100	0	0	100	0
Total = 96 scans								
%		44	55	41	46	7	57	43
Mean wavelength (nm)		380	419	463	569	625	639	656
(s.d.)		13	13	13	6	11	6	5
Metamorphosed Western Australian hosts								
Warrawoona 1 (chalced')	9	[1]*22	66	0	100	0	33	67
Warrawoona 1 (granular)	5	100	0	100	0	0	40	60
Killara 4	4	25	75	100	0	0	100	0
Killara 6	4	0	100	100	0	0	100	0
Maddina 1	4	0	100	0	100	0	50	50
Total = 26 scans								
%		31	65	50	50		58	42
Mean wavelength (nm)		387	423	476	560		643	653
(s.d.)		10	15	14	10		6	4

[1,2,3,4]* the prefix shows the number of outliers found outside the defined wavelengths for that particular Gaussian component.

Unpublished CL data (Table 4) from a previous study demonstrates the lack of any wavelength trends when an agate is systematically scanned N→S and W→E (Moxon and Reed, 2006). The discussion is based upon the relative peak intensities and the wavelengths obtained from three Gaussian components. Agate data are considered as three blocks: igneous hosts aged 13−1100 Ma; Stockdale Beck agates; and agates from the metamorphosed Western Australian hosts (Table 3).

Discussion

The age-related development in agate crystallinity is in part due to the metastable state of moganite. Three previous studies have used XRD to show that the moganite content of older microcrystalline quartz samples shows a decrease with age. Rodgers and Cressey (2001) found that the 20−200 ka old New Zealand sinters contain up to 13% moganite, although moganite was generally absent in the older Tertiary sinters. A collection of microcrystalline quartz from sedimentary environments only contained moganite in hosts that were younger than the Cretaceous (Heaney, 1995). Moganite was found in all agates from hosts younger than the Carboniferous but was found in only one of 32 tested agates from hosts aged 400 to 1100 Ma (Moxon and Ríos, 2004). However, moganite was identified in all agates from host rocks aged 400 to 1100 Ma when using Raman spectroscopy (Moxon *et al*., 2006). Furthermore, this Raman study also showed that moganite was absent from agates found in the 1.84−3.48 Ga metamorphosed hosts of Western Australia.

The greater sensitivity of Raman spectroscopy over XRD was first demonstrated by Götze *et al*. (1998). They also showed that the spatial resolution of Raman spectroscopy allowed the moganite in agate to be quantified band-to-band.

The present study used Raman spectroscopy to examine agates from Woolshed Creek, New Zealand (89 Ma), Northumbria, England (391 Ma), West Midland Valley, Scotland (412 Ma), Stockdale Beck (430 Ma) and Lake Superior, USA (1.10 Ga). Moganite was found in all samples except those from Stockdale Beck. In

TABLE 4. Emission bands identified in 16 scans on an agate from Chihuahua, Mexico.

		First Gaussian component		Second — Gaussian component —				Third Gaussian component	
		UV	Violet	Blue	Yellow	Orange		Orange	Red
		Wavelength range (nm)							
Chihuahua	Scan	340	400	451	540	591	Outlier	591	649
Mexico #2	no.	390	450	490	590	648		648	680
N→S scans	1	×					×		×
	2		×			×			×
	3		×		×				×
	4		×		×				×
	5		×			×			×
	6		×		×			×	
	7	×				×			×
W→E scans	8		×		×				×
	9		×		×				×
	10		×		×				×
	11		×		×				×
	12	×				×			×
	13		×		×				×
	14		×		×				×
	15		×		×				×
	16		×		×				×
Total = 16 scans									
%		19	81	0	69	25	6	6	94
Mean wavelength (nm)		376	410	–	562	612	444	643	660
(s.d)		13	6	–	4	14	–	–	5

agates of Devonian age and older, the intensity of moganite to α-quartz peak ratio showed little variation within an agate or band-to-band. However, the three Stockdale Beck agates together with the previously tested Western Australian agates were moganite-free and were indistinguishable from Brazilian macrocrystalline quartz (Fig. 6).

The Stockdale Beck agate locality is ~5 km from the outer limit of the metamorphic aureole around the Shap granite as given by Gale *et al.* (1979). Later data from a gravity survey allowed the production of topographic profiles across the Shap granite (Lee, 1986). One section profile, which is in the general direction of Stockdale Beck, gives an approximate depth of the granite dome near to Stockdale Beck of between 4 and 7 km. The increased crystallite growth in these Stockdale Beck agates could be the result of post-deposition heating due to the intrusion of the Shap granite. If this is the case then the subsequent heating has travelled through ~5 km of surrounding rock. Later heating is also shown by sediment deformation sequences that occurred over wide areas of the Lake District during the Devonian (Compston *et al*., 1982, and the literature cited therein).

Any moganite that was initially present in the Stockdale Beck agate has been transformed. In addition, these Stockdale Beck agates now have a crystallite size of ~60% greater than any other agate region in the 400−1100 Ma host-age range. It is suggested that late heating is the cause of this advanced growth over and above any moganite transformation.

The CI data from different studies have been used previously for comparison purposes (Kinnunen and Lindqvist, 1998). It has also been suggested that variation in the CI for similar materials in different studies could be due to the use of varied macrocrystalline quartz standards (Hattori *et al*., 1996). In this study, three different macrocrystalline standards produced minimal differences. However, comparisons from identical agate samples using different diffractometers produced different CI values. Direct CI comparisons should thus be made only when using the same model of diffractometer. Nevertheless, in this study we have examined five different samples of Stockdale Beck agate and these produced CI values of 9.7(0.1): this value is very close to the CI of agates from the Western Australian metamorphosed hosts and the macro-crystalline quartz standards. Additionally, the only samples to show a well developed 301 reflection were the macrocrystalline standards and agates from Western Australia and Stockdale Beck (Fig. 3).

There are few previous studies of agate using CL (Götze *et al*., 2001 and the literature cited therein). However, CL was used to show an age-related link between the healing of the defect causing the red emission band (~660 nm) and the increasing proportion of the orange emission band (~620 nm) (Moxon and Reed, 2006). It was shown that these changes occurred in both naturally occurring agate and laboratory-heated Brazilian agate. Here, it was proposed that the changes were due to a condensation reaction that occurred between neighbouring Si−OH groups forming a strained Si−O−Si bond (orange emission band). The present study has produced data showing the existence of two orange emission bands at ~620 nm (second Gaussian component) and ~640 nm (third Gaussian component). A non-bridging oxygen hole centre with a variety of precursors has been proposed as a possible cause for both of these bands (Stevens Kalceff and Philips, 1995 and references cited therein). The present study found an increase in the proportion of the 640 nm (orange) emission band over the 660 nm (red) emission band in the Stockdale Beck agates. This change supports previous suggestions that a condensation reaction occurs during heating with the loss of water from Si−OH groups.

The ~380 nm emission band has been attributed to a growth defect (Luff and Townsend, 1990). During the present study, the UV emission band at 380 nm has been found in both the heated agates of Stockdale Beck and the non-heated samples in approximately equal proportions, demonstrating that the defect is unaffected by heating. Luff and Townsend (1990) also attributed the blue luminescence in quartz to the decay of self-trapped excitons. This present study has identified an increase in the blue emission bands found in naturally heated agates (Table 3).

An earlier study was unable to detect differences between the relative intensities of red:violet:other colours shown by agates from different hosts or regions (Moxon and Reed, 2006). Consideration is given here to possible differentiation between naturally heated and unheated agates. Ternary plots have been used to examine permutations of the relative intensities between UV or violet: blue:red or orange. A clear distinction between the heated and unheated groups is shown with the

plot of violet:blue:orange. Apart from the Stockdale Beck agates, no single scan from 322 scans of agates in the 13–1100 Ma age group demonstrated this particular combination of defects. However, ~4% and 27% of respective separate scans on the Stockdale Beck and Western Australian agates were identified by this violet:-blue:orange combination (Fig. 8). The larger proportion of Western Australian samples is possibly a measure of more prolonged heating due to burial metamorphism.

A previous thermogravimetric study on the defect-site water content in agate from hosts aged 38 to 1100 Ma, demonstrated that the free water was independent of age, but water at defect sites showed an age-related decrease. After ~400 my, the defect site water had fallen from ~1% to become fixed at ~0.4% (Moxon and Ríos, 2004). For the present IR study, agates from Lake Superior (1100 Ma), West Midland Valley, Scotland (412 Ma) and Woolshed Creek, New Zealand (89 Ma) were compared with three Stockdale Beck agates. All these agates show free water (broad peak at 4000 to 2500 cm^{-1}). However, IR scans on all the Stockdale Beck samples show a near-zero silanol group at 3585 cm^{-1}. Some of the Western Australian samples also show some free water but the chalcedony in the oldest Warrawoona (sample no 1, 3.48 Ga) has almost zero free and silanol water (Fig. 5). This, together with the CL evidence, demonstrates that while the Stockdale Beck agates are able to lose and then recover the free water, the post-deposition heating has destroyed much of the silanol defect irreversibly.

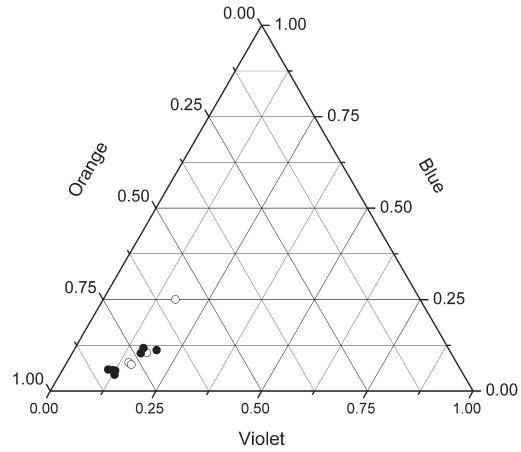

FIG. 8. A ternary plot showing the relative intensity of violet to blue to orange. This combination of defects has only been identified in single scans of agates from Stockdale Beck (open circles) and Western Australia (solid circles).

Previous studies on agates from the metamorphosed hosts in Western Australia allowed predictions about the likely heating effects on agate. Suggestions included: advanced grain growth accompanied by a well developed 301 quartz reflection; near-zero silanol water; and zero moganite. It was also suggested that a blue (~460 nm) emission band would be the only feature seen in the second Gaussian component. This has not been found but the blue emission band occurs much more frequently in the Stockdale Beck agates than in other agates of a similar age. The present study has confirmed the other characteristics of agate that have been subjected to post-deposition heating.

As far as we are aware, this is only the second study reporting advanced grain growth in agate caused by post-deposition heating. Examination of secondary-quartz infill found in the vicinity of later volcanic activity or within Archaean host rocks might identify the possibility of subsequent heating. Late heating can result in the total destruction of the characteristic agate banding. However, a thin-section examination could still identify some residual fibrosity. The use of Raman spectroscopy to search for moganite has proved particularly effective as moganite has been identified in all agates tested except those from Stockdale Beck and the metamorphosed hosts of Western Australia. On the basis of the evidence found in this study, a failure to detect moganite within chalcedonic fibrous textures is an indicator of palaeoheating.

Conclusion

The appearance of the Stockdale Beck agates suggests a contemporaneous deposition of host and agate. However, the characterized properties are neither due to the age of the agate nor the ignimbrite host rock. It is proposed that the Stockdale Beck agates have been subjected to post-deposition heating that has altered their character. Possible heat sources include the later Shap granite intrusion or later sediment deformation activity during the Devonian. The present study of the Stockdale Beck agates has shown that:

(1) Some samples contain an unusual region of milky macrocrystalline quartz, but IR spectroscopy shows that the silanol water content in the agates is near zero.

(2) Thin sections reveal an atypical fibrous texture.

(3) The mean crystallite size ($C_{s(101)}$) is ~60% greater than would be expected from agates of this host-rock age. However, these agates have not reached the advanced crystallinity shown by agates from the metamorphosed hosts of Western Australia.

(4) The assessment of quartz crystallinity using the Crystallinity Index has limitations, particularly if different diffractometers are employed. Nevertheless, the CI of the Stockdale Beck agates determined in this study is close to that of the Brazilian macrocrystalline quartz reference.

(5) A well developed 301 reflection has only been found in macrocrystalline quartz, and in Stockdale Beck and Western Australian agates.

(6) They contain zero moganite.

(7) They produce a high proportion of the blue CL emission band (~470 nm).

Acknowledgements

We are obliged to the Department of Earth Sciences, Cambridge University; to Michael Carpenter for helpful discussions during this study, and to Andy Buckley for comments on the paper. Ian Marshall gave assistance with the SEM and Tony Abraham helped with the XRD data collection. The full agate study has relied on the generous donation of agate by collectors and research workers from around the world. We are indebted to Rob Burns, Jeanette Carrillo , Roger Clark, Nick Crawford, Brad Cross, Robin Field, Gerhard Holzhey, Brian Isfeld, Herbert Knuettel, Reg Lacon, Brian Leith, Maziar Nazari, Dave Nelson, Leonid Neymark, John Raeburn, John Richmond, Vanessa Tappenden, Bill Taylor, Bill Wilson, Scott Wolter and Johann Zenz. We are particularly grateful to Robin Field for showing TM the Stockdale Beck site.

Stockdale Beck is now a Site of Special Scientific Interest and permission to collect here is required from the Lake District National Park Authority, Natural England and the local landowners. We are much obliged to Sue Thompson and Ian Clement from LDNPA, Simon Webb (NE), Richard Simpson, Hal Bagot, Paul Phillips (United Utilities) for permission to explore the area and collect a limited number of samples. We are also obliged to two anonymous reviewers for their constructive and helpful comments after a first submission of the manuscript. TM thanks The Leverhulme Trust for the financial support.

References

Barley, M.E., Weaver, S.D. and de Laeter, J.R. (1988) Strontium isotope composition and geochronology of intermediate-silicic volcanics, Mt Somers and Banks Peninsula, New Zealand. *New Zealand Journal of Geology and Geophysics*, **31**, 197–206.

Bish, D.L. and Reynolds, R.C., Jr. (1989) Sample preparation for X-ray diffraction. Pp. 73–99 in: *Modern Powder Diffraction* (D.L. Bish and J.E. Post, editors). Reviews in Mineralogy, **20**, Mineralogical Society of America, Washington D.C.

Braitsch, O. (1957) Über die natürlichen Faser-und Aggregationtypen beim SiO_2, ihre Verwachsungsformen, Richtungsstatistik und Doppelbrechung. *Heidelberger Beiträge zur Mineralogie und Petrographie*, **5**, 331–372.

Cady, S.L., Wenk, H.-R. and Sintubin, M. (1998) Microfibrous quartz varieties: characterization by quantitative X-ray texture analysis and transmission electron microscopy. *Contributions to Mineralogy and Petrology*, **130**, 320–335.

Compston, W., McDougall, I. and Wyborn, D. (1982) Possible two-stage ^{87}Sr evolution in the Stockdale Rhyolite. *Earth and Planetary Science Letters*, **61**, 297–302.

Flörke, O.W., Köhler-Herbertz, B., Langer, K. and Tönges, I. (1982) Water in microcrystalline quartz of Volcanic Origin: Agates. *Contributions to Mineralogy and Petrology*, **80**, 324–333.

Frondel, C. (1978) Characters of quartz fibers. *American Mineralogist*, **63**, 17–27.

Gale, N.H., Beckinsale, R.D. and Wadge, A.J. (1979) A Rb-Sr whole rock isochron for the Stockdale Rhyolite of the English Lake District and a revised mid-Palaeozoic time-scale. *Journal of the Geological Society, London*, **136**, 235–242.

Götze, J., Nasdala, L., Kleeberg, R. and Wenzel, M. (1998) Occurrence and distribution of 'moganite' in agate/chalcedony: a combined micro-Raman, Rietveld, and cathodoluminescence study. *Contributions to Mineralogy and Petrology*, **133**, 96–105.

Götze, J., Plötze, M. and Habermann, D. (2001) Origin, spectral characteristics and practical applications of the cathodoluminescence (CL) of quartz – a review. *Mineralogy and Petrology*, **71**, 225–250.

Graetsch, H., Flörke, O.W. and Miehe, G. (1985) The nature of water in chalcedony and opal-C from Brazilian agate geodes. *Physics and Chemistry of Minerals*, **12**, 300–306.

Hattori, I., Umeda, M., Nakagawa, T. and Yamamoto, H. (1996) From chalcedonic chert to quartz chert: diagenesis of chert hosted in a Miocene volcanic-sedimentary succession, Central Japan. *Journal of Sedimentary Research*, **66**, 163–174.

Heaney, P.J. (1995) Moganite as an indicator for

vanished evaporates: a testament reborn? *Journal of Sedimentary Research*, **A65**, 633–638.

Holzhey, G. (1999) Mikrokristalline SiO_2-Mineralisationen in rhyolithischen Rotliegendvulkaniten des Thüringer Waldes (Deutschland) und ihre Genese. *Chemie der Erde*, **59**, 183–205.

Keller, P.C., Bockoven, N.T. and McDowell, F.W. (1982) Tertiary volcanic history of the Sierra del Gallego area, Chihuahua, Mexico. *Geological Society of America Bulletin*, **93**, 303–314.

Kingma, K.J. and Hemley, R.J. (1994) Raman spectroscopic study of microcrystalline quartz. *American Mineralogist*, **79**, 269–273.

Kinnunen, K.A. and Lindqvist, K. (1998) Agate as an indicator of impact structures: an example from Sääksjärvi, Finland. *Meteoritics and Planetary Science*, **33**, 7–12.

Klug, H.P. and Alexander, L.E. (1974) *X-ray Diffraction Procedures for Polycrystalline and Amorphous Materials.* John Wiley and Sons, New York.

Lee, M.K. (1986) A new gravity survey of the Lake District and three-dimensional model of the granite batholith. *Journal of the Geological Society, London*, **143**, 425–435.

Lange, P., Blankenburg, H.-J. and Schrön, W. (1984) Rasterelektronmikroskopische Untersuchungen an Vulkanachaten. *Zeitschrift für Geologische Wissenschaften*, **12**, 669–683.

Luff, B.J. and Townsend, P.D. (1990) Cathodoluminescence of synthetic quartz. *Journal of Physics of Condensed Matter*, **2**, 8089–8097.

Miehe, G. and Graetsch, H. (1992) Crystal structure of moganite: a new structure type for silica. *European Journal of Mineralogy*, **4**, 693–706.

Millward, D. and Lawrence, D.J.D. (1985) The Stockdale (Yarlside) Rhyolite – a rheomorphic ignimbrite? *Proceedings of the Yorkshire Geological Society*, **45**, 299–306.

Moxon, T. (1991) On the origin of agate with particular reference to fortification agate found in the Midland Valley, Scotland. *Chemie der Erde*, **51**, 251–260.

Moxon, T. (2002) Agate: a study of ageing. *European Journal of Mineralogy*, **14**, 1109–1118.

Moxon, T. and Ríos, S. (2004) Moganite and water content as a function of age in agate: an XRD and thermogravimetric study. *European Journal of Mineralogy*, **16**, 269–278.

Moxon, T. and Reed, S.J.B. (2006) Agate and chalcedony from igneous and sedimentary hosts aged 13 to 3480 Ma: a cathodoluminescence study. *Mineralogical Magazine*, **70**, 485–498.

Moxon, T., Nelson, D.R. and Zhang, M. (2006) Agate recrystallization: evidence from samples found in Archaean and Proterozoic host rocks, Western Australia. *Australian Journal of Earth Sciences*, **53**, 235–248.

Murata, K.J. and Norman II, M.B. (1976) An index of crystallinity for quartz. *American Journal of Science*, 276, 1120–1130.

Nelson, D.R., Trendall, J.R., de Laeter, J.R., Grobler, N.J. and Fletcher, I.R. (1992) A comparative study of the geochemical and isotropic systematics of late Archaean flood basalts from the Pilbara and Kaapvaal cratons. *Precambrian Research*, **54**, 231–256.

Parthasarathy, G., Kunwar, A.C. and Srinivasan, R. (2001) Occurrence of moganite-rich chalcedony in the Deccan flood basalts, Killari, Maharashtra, India. *European Journal of Mineralogy*, **13**, 127–134.

Pop, D., Constantina, C., Tătar, D. and Kiefer, W. (2004) Raman spectroscopy on gem-quality microcrystalline and amorphous silica varieties from Romania. *Geologia*, **XLIX**, 1, 41–52.

Rodgers, K.A. and Cressey, G. (2001) The occurrence, detection and significance of moganite (SiO_2) among some silica sinters. *Mineralogical Magazine*, **65**, 157–167.

Stevens Kalceff, M.A. (1998) Cathodoluminescence microcharacterization of the defect structure of irradiated hydrated and anhydrous fused silicon dioxide. *Physical Review B*, **57**, 5674–5683.

Stevens Kalceff, M.A. and Philips, M.R. (1995) Cathodoluminescence microcharacterization of the defect structure of quartz. *Physical Review B*, **52**, 3122–3134.

Wadge, A.J., Gale, N.H., Beckinsale, R.D. and Rundle, C.C. (1978) A Rb-Sr isochron for the Shap granite. *Proceedings of the Yorkshire Geological Society*, **42**, 297–305.

Yamagishi, H., Nakashima, S. and Ito, Y. (1997) High temperature infrared spectra of hydrous microcrystalline quartz. *Physics and Chemistry of Minerals*, **24**, 66–74.